

Electrical And Dielectric Properties Of M-Type Strontium Hexaferrites Doped With Gd-Rare Earth Ions

^aArun Katoch, ^bAnterpreet Singh, ^cTaminder Singh

^aDepartment of Physics, Singhania University, Rajasthan, India

^bDepartment of Applied Sciences, BKSJ Engg. College, Amritsar, India

^cDepartment of Physics, Khalsa College, Amritsar, India.

ABSTRACT

A series of hexagonal ferrite samples with the composition of $Sr_{1-x}Gd_xFe_{12}O_{19}$ ($x = 0.0, 0.10, 0.20, 0.30$ and 0.40) have been prepared by employing the ceramic technique. The structural properties of the calcined samples were studied using X-ray diffraction (XRD), SEM technique. The samples were sintered at $1150^\circ C$ for 8 hours. The X-ray diffraction patterns shows that the prepared samples have a single phase and the effect of composition on the unit cell parameters, density and porosity has been studied. The lattice parameters 'c' and 'a' was found to decreases by increasing Gd-content whereas the X-ray density increases by increasing Gd-content. Microstructural analysis by scanning electron microscopy (SEM) suggest that the compound have small grains distributed uniformly and non-uniformly on the surface of the sample and also shows that the grain size has been decreased by increasing the Gd-content in the composition $Sr_{1-x}Gd_xFe_{12}O_{19}$. The variation of AC conductivity (σ_{AC}) with frequency ranging from 1KHz to 1MHz shows that the electrical conductivity in these ferrites is mainly due to electron hopping mechanism. The variation of dielectric constant (ϵ') and loss tangent ($\tan\delta$) in the frequency range 1KHz to 1MHz was studied. The conduction phenomenon on was explained on the basis of a small polaron hopping model.

Keywords: Hexagonal ferrites, X-ray diffraction, SEM, AC conductivity (σ_{AC}) and dielectric constant (ϵ')

1. Introduction

Low cost, easily manufacturing and interesting electric and magnetic properties lead the polycrystalline ferrite to be one of the most important material that has attracted a considerable attention in the field of technological application in a wide range of frequency extended from microwave to radio frequency. Their electrical and dielectric properties depends on the preparation condition, such as sintering temperature, sintering atmosphere and the soaking time as well as the type of the substituted ions. It was proposed that the air-sintered ferrites are characterized by microstructure consisting of relatively high conductive grains separated by high resistive grain boundaries [1-2]. Hexagonal barium ferrites have been intensively investigated during the last few decades due to their considerable importance to the electronic material industry. The hexagonal Barium ferrite (BaM) is considered to be an excellent candidate for magnetic recording media and characterized with high magnetocrystalline anisotropy, moderate hard magnetic properties and high chemical stability, compared with other magnetic materials [3-6].

The common processing methods of hexagonal ferrites are conventional ceramic process of solid-state reaction[7],

co-precipitation method[8], sol-gel process[9] and molten salt method [10,11] etc. The conventional ceramic process, which includes the mixing the raw materials, calculation, milling, pressing and sintering at $1200-1350^\circ C$ [12]. In a fine particle form, barium ferrite is suitable for high-density recording media. Ultrafine barium ferrite powder with narrow particle size distribution is desirable to increase the capacity of information storage as well as to reduce the medium noise [13].

The paper aims at synthesizing Gd substituted SrM hexaferrite by conventional ceramic technique and study effect of Gd ion substitution on the electrical, dielectric and structural properties and particle size of hexaferrite were investigated by XRD, SEM.

2. Experimental

2.1. Preparation of the samples

The hexagonal barium ferrites of nominal composition ($x = 0.0, 0.10, 0.20$ and 0.30) were synthesized starting from ball-milling mixtures of SrCO_3 , Fe_2O_3 and Gd–rare earth ion for 12h. After drying at 60°C for 6h, the powder mixture was heated at temperature of $800\text{--}1150^\circ\text{C}$ for 4 h in a lid –covered alumina crucible with a heating rate of $5^\circ\text{C}/\text{min}$ in air. Then after cooling to room temperature in furnace. In order to make the sintered magnet, the Strontium ferrite powder were wet mixed in acetone medium with addition of 4% polyvinyl alcohol (PVA) binder solution by using a ball mill. The mixture were reground again for 5h and the final fine powder were pressed in disk-shaped pellets with thickness ranging from 2mm to 4mm and with diameter from 7mm to 9mm. Then the pellets were sintered in a resistance heated furnace for 3h at each specified level of sintering temperature from 950 to 1150°C . The samples were slowly cooled to room temperature. Finally, the surfaces of the disk were polished and coated by silver paste that act as a good contact for measuring the electric and dielectric properties.

2.2. Measurements details

Structural characterization was carried out by X-ray diffraction (XRD), Scanning electron microscope (SEM). The crystal structure of the samples was examined by using a X-ray diffractometer (XPRT-PRO) with CuK_α ($\lambda = 1.5406$) radiations. The microstructure was investigated using scanning electron microscope (SEM, JEOL-JSM 6100). The DC electrical conductivity (σ) of all the samples was measured at room temperature by two probe method. The specimen was connected through a dry battery of 1.5 to 3 V Keithley electrometer (Model 6517A), for measuring the current.

The DC conductivity was calculated by using the formula

$$\sigma = \frac{It}{VA} \quad (1)$$

where I is the current passing through the specimen in amperes, V is the voltage applied to the specimen in volts, t is the thickness of the sample in cm and A denotes the cross-sectional area of the sample in cm^2 .

A study of the variation of AC electrical conductivity with frequency and temperature has been carried out by the two-probe method. The conductivity cell used for the measurement of electrical conductivity. The AC conductivity was calculated by using the relation

$$\sigma_{AC} = \frac{Gt}{A} \quad (2)$$

where t and A are the thickness and area of cross-section of the sample and G is the conductance. The value of dielectric constant (ϵ') of the ferrite samples can be calculated by using the formula

$$\epsilon' = \frac{C_{pt}}{\epsilon_0 A} \quad (3)$$

[thickness of the samples in cm, A is the cross-sectional area of the sample in cm^2 and ϵ_0 is the permittivity in free space having value 8.854×10^{-2} pF/cm.

3. Result and discussion

3.1 Phase Identification

Fig. 1 shows the XRD pattern obtained for different molar concentration in the prepared samples of $\text{Sr}_{1-x}\text{Gd}_x\text{Fe}_{12}\text{O}_{19}$ ferrites sintered at 1150°C for 3h. In Gd^{+3} series, all peaks corresponds to hexagonal M-type phase. However, for the substitution $X = 0.30$, a weak peak characteristic of the hematite ($\alpha\text{-Fe}_2\text{O}_3$) phase is observed, indicating that the sample contains a slight proportion of $\alpha\text{-Fe}_2\text{O}_3$. This indicate that This indicates that Gd for $x = 0.30$ did not substitute totally into the Sr M-type structure resulting in incomplete reactions between Fe^{3+} and Sr^{2+} , indicated by tracing of secondary phases in these samples, and is attributed to the preparation process. The respective peaks show that a magnetoplumbite structure has been formed. The variation in relative intensities of peaks may be related to the occupation of lattice sites by substituted ions. The lattice constants 'a' and 'c' with composition (x) for $\text{Sr}_{1-x}\text{Gd}_x\text{Fe}_{12}\text{O}_{19}$ has been decreases continuously with increasing substituted amount of Gd ions. The peaks for the doped Strontium ferrites appear at the same position as for undoped ferrite, with different intensities. The result indicates that the formation of temperature of $\text{Sr}_{1-x}\text{Gd}_x\text{Fe}_{12}\text{O}_{19}$ is about 1150°C . It is about 50°C higher than that of classical ceramic method for undoped strontium ferrite as indicated in the literatures. In the doped ferrites cases, the dopant of Gd^{2+} seem to dissolve / arrange in the hexagonal structure to fulfill the formation of single hexagonal phase[14].

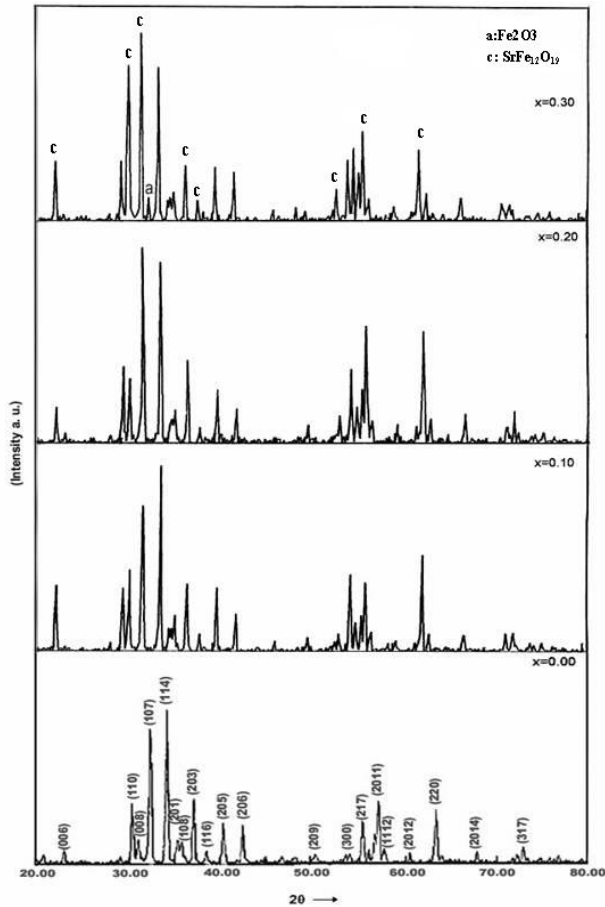


Fig. 1. XRD Patterns of $\text{Sr}_{1-x}\text{Gd}_x\text{Fe}_{12}\text{O}_{19}$ for compositions (a) $X=0$, (b) $X=0.10$, (c) $X=0.20$ and (d) $X=0.30$

3.2. SEM Microstructures

Fig. 2. shows the microstructures of prepared samples. It indicates that the M-type ferrite grains are homogeneous hexagonal shaped crystals [14]. It was found that the average grain size estimated from SEM was approximately $1\mu\text{m}$ and it was almost dependent on the composition X ($x=0.0$, 0.10 , 0.20 and 0.30). The complex permeability spectra of polycrystalline ferrite depends not only on the chemical composition of the ferrite but also on the post-sintering density and the microstructures such as grain size and porosity.

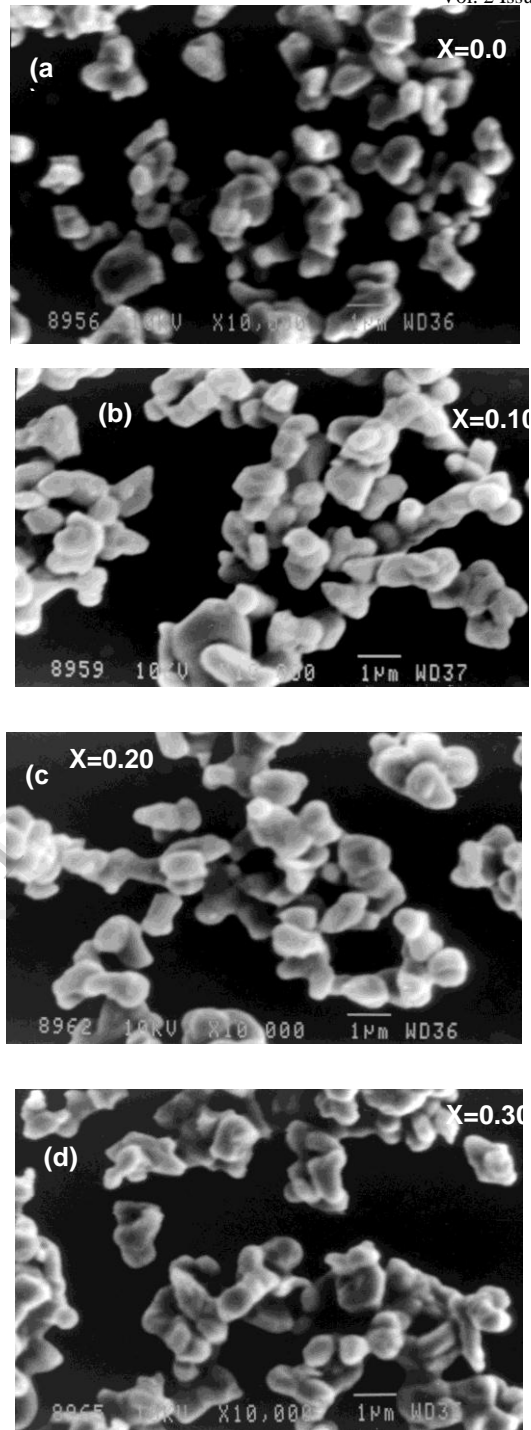


Fig. 2. SEM Photographs of $\text{Sr}_{1-x}\text{Gd}_x\text{Fe}_{12}\text{O}_{19}$ for compositions (a) $X=0$, (b) $X=0.10$, (c) $X=0.20$ and (d) $X=0.30$

3.3 AC conductivity

Fig. 3. shows the variation of the real part of AC conductivity σ' with temperature at different selected frequencies for the prepared compositions of $Sr_{1-x}Gd_xFe_{12}O_{19}$ ($X=0, X=0.10, X=0.20$ and $X=0.30$). Fig. 4. shows the frequency dependence of real part of AC conductivity σ' for all the samples at different temperatures. It is shown that for $Sr_{1-x}Gd_xFe_{12}O_{19}$ sample (where $X=0.0$), the dispersion of AC conductivity at low temperature and relatively high frequency region. With replacement of Fe^{3+} ions by Gd^{3+} ions, the dispersion region is shifted towards relatively lower frequencies. Generally, the dispersion of AC conductivity decreases with increasing the temperature for all samples. At relatively high temperature the AC conductivity seems to be frequency independent. The results of AC conductivity σ' can be explain on the basis of the assumption that σ' can be expressed as [15]

$$\sigma' = \sigma_{DC} + \sigma_{AC} \quad (4)$$

where the first term is a temperature dependent term represent the DC electric conductivity which is related to drift mobility of the free charge carriers, and the second term is a frequency and temperature dependent term which is related to the dielectric relaxation of the bound charge carriers. The first term is predominant at low frequencies and high temperature, while the second term is predominant at high frequencies and low temperature. The results of plot of $\log \sigma_{AC}$ against $10^3/T$ show that σ_{AC} exhibits a semi-conductive behaviour with the temperature, where the AC conductivity increases with increasing temperature. The results of AC conductivity could be explained on the basis of Koops Model, which assumes that ferrite samples act as a multilayer capacitor in which the ferrite grain and grain boundaries have different properties. According to this model, the bulk material of the ferrite could be considered as consisting two layers, one represents the grains (a conducting layer) and the other represents the grain boundaries (a poor conducting layer). The grain have high conductivity are effective at high frequencies. However the grain boundaries have low conductivity and are effective at lower frequencies.

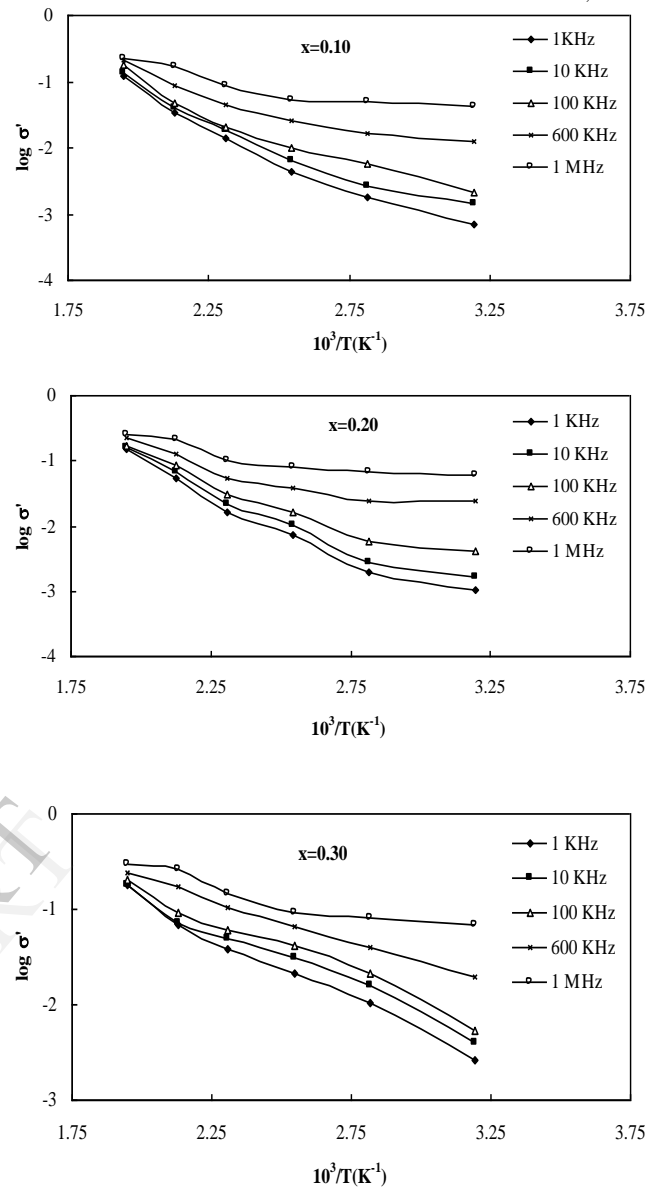
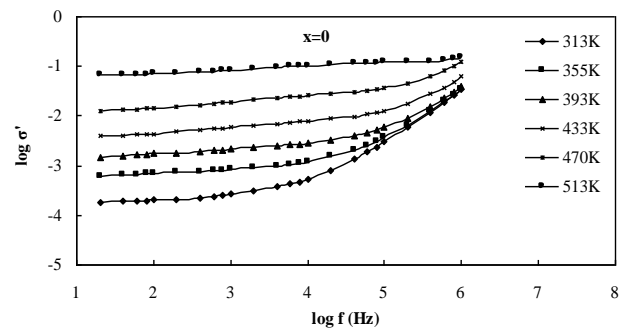
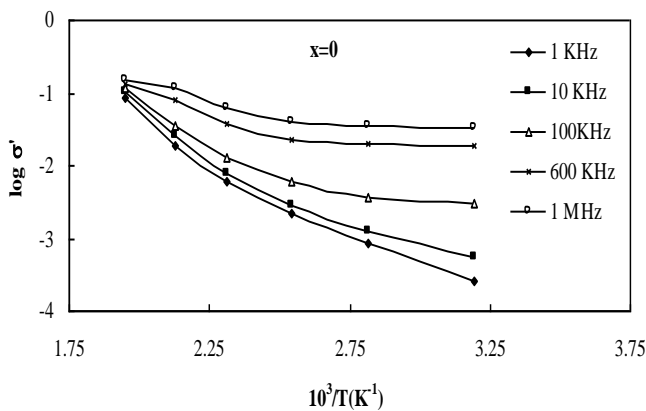


Fig. 3. Temperature dependance of AC conductivity of $Sr_{1-x}Gd_xFe_{12}O_{19}$ at different frequencies.



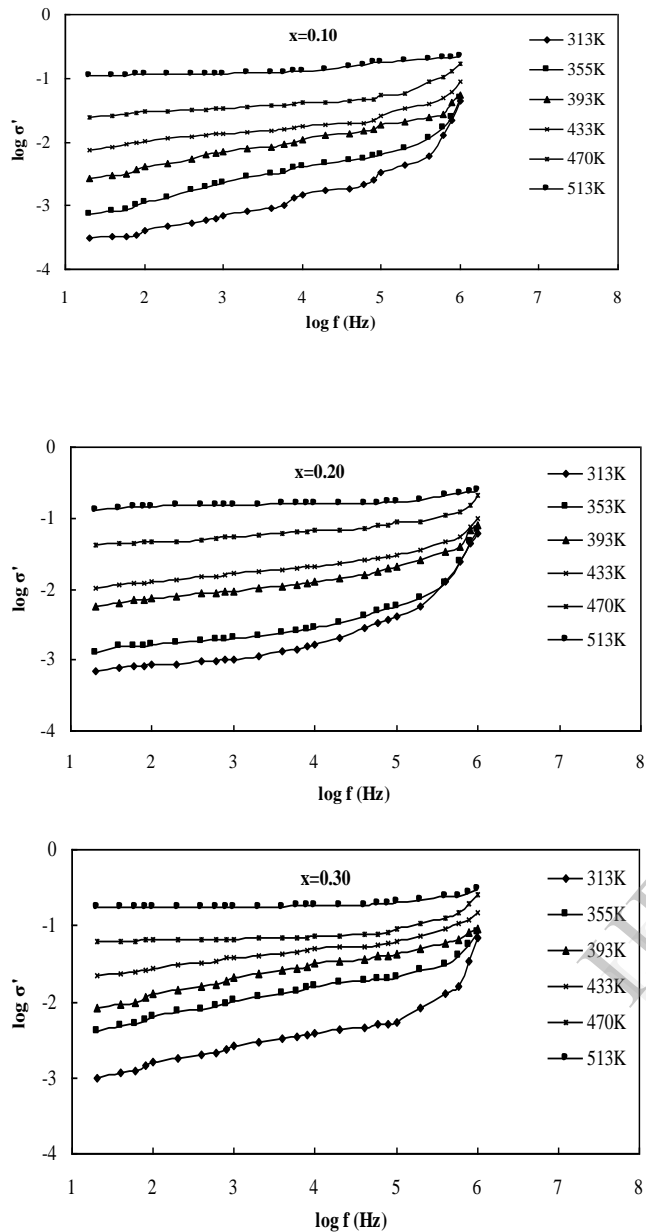


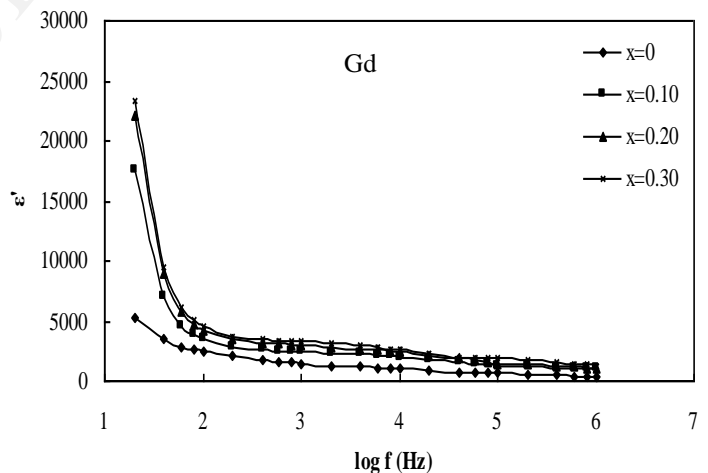
Fig. 3. Frequency dependance of AC conductivity of $Sr_{1-x}Gd_xFe_{12}O_{19}$ at different temperatures.

3.4 Dielectric properties

The variation of dielectric constant with frequency is shown in Fig.7 The dielectric constant decreases with increasing frequency. This behaviour in rare earth substituted Sr hexaferrites is a common ferrimagnetic behaviour and also been observed by other investigator [16-18]. A more dielectric dispersion is observed at lower frequency range and it remains almost independent of applied external field at high frequency domain. This is due to the fact that dielectric material exhibit induced electric moment under the influence of external electric field. At higher frequency, the polarization of the induced moment could not synchronize with the frequency of applying electric field. So dielectric attains a constant value above certain high frequencies. [19]. The polarization is governed by number of space charge carriers while take part bin the ion exchange during the hopping phenomenon in $Fe^{3+} - Fe^{2+}$

or $Gd^{3+} - Gd^{2+}$ may be produced during the sintering process due to production of oxygen ion vacancies, that make the phenomenon of hopping more easier[20-25]. The dielectric dispersion is observed at low frequency – range is due to Maxwell-Wagner type interfacial polarization well in agreement with the Koops phonological theory[1],[26, 27] . According to these models, the dielectric material with a heterogeneous structure can be imagined as a structure consist of well conducting grains separated by highly resistive thin layer (grain boundaries). In this case, the applied voltage on he sample drops mainly across the grain boundaries and space charge polarization is built up at the grain boundaries.

The space charge polarization is governed by the available free charges on the grain boundaries and grain boundaries is predominant at low frequencies. The thinner the grain boundary, the higher the dielectric constant. The observed decrease of ϵ' with increasing the frequency can be attributed to the fact that the electron exchange between Fe^{2+} and Fe^{3+} ions can not follow the change of the external applied field beyond a certain frequency [21]. Basically, the whole polarization in ferrites is mainly contributed by the space charge polarization which is governed by the space charge carriers and the conductivity of material.[22-23] and hopping exchange of charge between two localized states, which is governed by the density of the localized states and resultant displacement of these charges with respect to the external field.



Conclusion

$Sr_{1-x}Gd_xFe_{12}O_{19}$ hexaferrite are prepared by the usual ceramic technique. From the above study, we conclude that the X-ray diffraction pattern shows that the prepared samples have a single phase structure. The lattice parameters 'c' and 'a' was found to decreases by increasing Gd-content, that enhanced the X-ray density and porosity. SEM suggested that the compound have small grains distributed on the surface of the sample and also shows the grain size has been decreases by increasing the Gd-content in the composition $Sr_{1-x}Gd_xFe_{12}O_{19}$. The result of AC electric conductivity with frequency were explained on the basis of the hopping conduction mechanism and space charge polarization discussed by Maxwell- Wanger and

Koop's models. The dielectric constant decreases with increasing frequency. The value of dielectric constant at relatively at low frequency were very high and are attributed to the existence of interfacial polarization that arises due to in homogeneous structure of the material ensuring the presence of the secondary phases at the grain boundaries.

References

- [1] Koops, C.G., *phys.Rev.*83(1951)121
- [2] A. Dias, R.Luiz Moreire, *J. Mater. Res.* 12 (8) (1998) 2190
- [3] Shuki Yamamoto, Xioxi Liu, Akimitsu Morisako, *jmmm* 316(2007)e152-e154
- [4] T.Gonzalez-Carreno, M.P.Morales, C.J. Serna. *Mater. Lett.* 43 (2000)
- [5] A.Morisaka, M. Matsumato, M. Naoe, *J. Magn. Mater.* 54-57(1985) 1657
- [6] X. Sui, M.h. Kryder, B.Y. Wong, D.E. Laughlin, *IEEE trans.* 29(1993) 3751
- [7] F.Harberey, A. Kockel, *IEEE Trans. Magn.* 12 (1976) 983
- [8] J.H. Lee, H.H. Lee, C.W. Won, *J.Kor. Inst.Met. Mater.* 33(1995)21
- [9] H.Zhang, L.Li, J.Zhou, Yue, Z. Ma, Z. Gui, *J. Eur. ceram. Soc.* 21(2001)149
- [10] Y. Hayashi, T.Kanazawa, T. Yamaguchi,, *J.mater.Sci.*21(1986)2876
- [11] T. Kimura, T. Takahashi, T. Yamaguchi, *J.Mater. Sci.* 15(1980)1491
- [12] Si-Dong Kim, Jung -Sik Kim. *Mater.* 307(2006) 295-300
- [13] T. Gonzalez-Carreno, M.P. Morales, C.J. Serna, *Mater. Lett.* 43 (2000) 97
- [14] A.Ghasemi, A.Hossienpour,A.Morisako,A.Saatchi, M.Salehi, *jmmm*.303(2006)429-435
- [15] Y. Yamazaki, M. Satou, *Jpn.J.Appl. Phys.* 12(7) (1973) 998
- [16] Ravinder, D., Vijaya, P and Reddy, B., *Mater. Lett.*, **57**, 4344 (2003).
- [17] Shaikh, A.M., Belled, S.S and Chougule, B.K., *J. Magn. Mater.*, **195**, 384 (1999).
- [18] Kumar, B.R and Ravinder, D., *Mater. Lett.*, **53**, 437 (2002).
- [19] H.V. Keer, *Principal of Solid state*, new Age Int. pub.LTD.,Mumbai,2000.
- [20] K.W.Wagner,*Ann.Phys.*40(1913),817
- [21] V.R. K. Murthy. *J. Sobhamadri, Phys. Status Solidi* A36(1976)1233.
- [22] C.Parakash .J.S .Baijal . *Less-Common Met* 107(2006) 51
- [23] B.K.Kuanr, G.P.S. Tara, *Appl.Phys.* 75(10) 2001, 6115.
- [24] A.K. Jonscher, *Dielectric Relaxation in Solids*, Chelsea Dielectrics Press, London, 1982
- [25] J.Maexwell, *Electricity and Magnetism*, Vol 1, Oxford University Press, London, 1873
- [26] Maxwell, J.C., "Electricity and Magnetism", (Oxford)University Press, London, (1873).
- [27] Wagner, K.W., *Ann. Phys.*, **40**, 817 (1973).